

# Double ionization of nitrogen molecules in orthogonal two-color femtosecond laser fields

Qiyong Song<sup>1</sup> , Hui Li<sup>1,4</sup>, Junping Wang<sup>2</sup>, Peifen Lu<sup>1</sup>, Xiaochun Gong<sup>1</sup> ,  
Qinying Ji<sup>1</sup>, Kang Lin<sup>1</sup>, Wenbin Zhang<sup>1</sup>, Junyang Ma<sup>1</sup>, Hanxiao Li<sup>1</sup>,  
Heping Zeng<sup>1</sup>, Feng He<sup>2,4</sup> and Jian Wu<sup>1,3</sup>

<sup>1</sup> State Key Laboratory of Precision Spectroscopy, East China Normal University, Shanghai 200062, People's Republic of China

<sup>2</sup> Key Laboratory of Laser Plasmas (Ministry of Education) and Department of Physics and Astronomy, Collaborative Innovation Center for IFSA (CICIFSA), Shanghai Jiao Tong University, Shanghai 200240, People's Republic of China

<sup>3</sup> Collaborative Innovation Center of Extreme Optics, Shanxi University, Taiyuan, Shanxi 030006, People's Republic of China

E-mail: [hli@lps.ecnu.edu.cn](mailto:hli@lps.ecnu.edu.cn) and [fhe@sjtu.edu.cn](mailto:fhe@sjtu.edu.cn)

Received 6 December 2017, revised 21 January 2018

Accepted for publication 22 February 2018

Published 16 March 2018



CrossMark

## Abstract

Double ionization of nitrogen molecules in orthogonally polarized two-color femtosecond laser fields is investigated by varying the relative intensity between the fundamental wave (FW) and its second harmonic (SH) components. The yield ratios of the double ionization channels, i.e., the non-dissociative  $N_2^{2+}$  and Coulomb exploded ( $N^+$ ,  $N^+$ ), to the singly charged  $N_2^+$  channel exhibit distinct dependences on the relative strength between the FW and SH fields. As the intensity ratio of SH to FW increases, the yield ratio of  $(N^+, N^+)/N_2^+$  gradually increases, while the ratio of  $N_2^{2+}/N_2^+$  first descends and then increases constituting a valley shape which is similar to the behavior of  $Ar^{2+}/Ar^+$  observed in the same experimental condition. Based on the classical trajectory simulations, we found that the different characteristics of the two doubly ionized channels stem from two mechanisms, i.e., the  $N_2^{2+}$  is mostly accessed by the  $(e, 2e)$  impact ionization while the recollision-induced excitation with subsequent ionization plays an important role in producing the  $(N^+, N^+)$  channel.

Keywords: strong-field physics, two-color femtosecond laser pulses, electron–ion recollision, molecular dynamics

(Some figures may appear in colour only in the online journal)

## 1. Introduction

As one of the most important electron-recollision-related phenomena when atoms and molecules interacting with strong laser fields, the nonsequential double ionization (NSDI) has been intensively investigated for more than three decades [1]. Enormous efforts have been made for the exploration of the unexpected enhanced double ionization rate [2–4], the correlated dynamics of two freed electrons of their

momenta and kinetic energies [5–10], and so on. The underlying physics of NSDI is generally understood with a scenario of electron-recollision-assisted three-step process [11, 12]. According to this picture, NSDI can occur via two routes, i.e., the  $(e, 2e)$  impact ionization and the recollision-induced excitation with subsequent ionization (RESI), depending on the returning energy of the rescattered electrons [9, 13].

As compared to the double ionization in atoms, different channels can be accessed in the double ionization of molecules, e.g., the non-dissociative double ionization channel, and the charge symmetric and asymmetric dissociative

<sup>4</sup> Authors to whom any correspondence should be addressed.

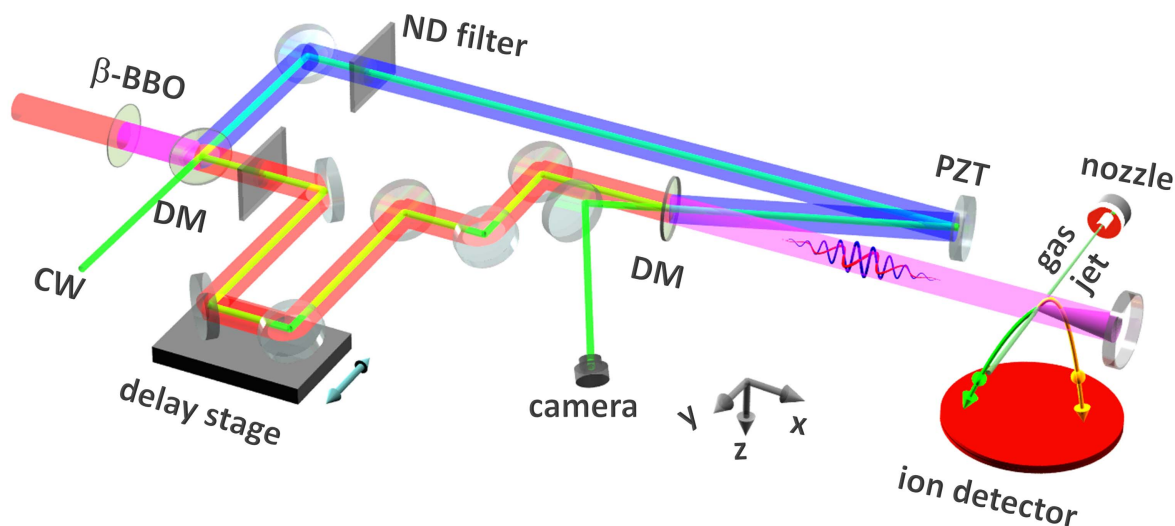


**Figure 1.** Scheme of the experimental setup. In the figure, DM stands for dichroic mirror,  $\beta$ -BBO stands for  $\beta$ -barium borate crystal, PZT stands for piezo-based delay stage, CW stands for continuum-wave laser at 532 nm, and ND filter stands for neutral density filter.

channels. The distinct molecular double ionization channels can be accessed via different routes owing to the complexity of the detailed electronic and nuclear structures of various molecules [14–16]. For example, for the double ionization of  $N_2$ , the previous study [14] shows that the  $N^{2+} + N$  channel is mainly produced via the NSDI, but the  $N^+ + N^+$  channel is dominated by the sequential double ionization (SDI). However, for another heteronuclear diatomic molecule CO, it is demonstrated that the  $C^{2+} + O$  channel following the double ionization is mainly accessed via the SDI [17, 18].

The two-color ultrashort laser pulses perform as a powerful tool in controlling the ultrafast dynamics of molecules by finely tuning the relative phase between the fundamental wave (FW) and its second harmonic (SH) components. Comparing to the colinearly polarized two-color laser fields, the orthogonally polarized two-color (OTC) laser fields allow one to manipulate the launching and propagation of electronic and nuclear wave packets in ultrahigh spatiotemporal precision [19, 20]. The OTC pulses have been used to increase the generation efficiency [21], to control the polarization state of high-harmonic radiation [22], and to visualize the atomic and molecular orbitals [23, 24]. OTC fields have been used to steer the laser-induced electron diffraction [25], the correlated dynamics of the released electrons in the double ionization of atoms [10, 26], the directional breaking of molecular bond in two-dimensional space [27–29], and to reveal attosecond Freeman resonance time delay [30] and non-adiabatic dynamics [31] of the photoelectron emission. Here, we investigate the double ionization of  $N_2$  molecules and Ar in OTC femtosecond laser fields, in particular the different double ionization pathways towards various channels as a function of the relative intensity between the FW and its SH components.

## 2. Experimental setup

The experimental measurements were performed in a standard reaction microscope of cold target recoil ion momentum

spectroscopy [32, 33]. As illustrated in figure 1, a beam of linearly polarized femtosecond laser pulses (25 fs, 790 nm, 10 kHz) delivered from a multipass amplifier Ti:sapphire laser was down-collimated into a 150  $\mu\text{m}$  thick  $\beta$ -barium borate crystal to generate the SH pulses at 395 nm. The FW and SH pulses were then separated by a dichroic mirror, whose intensities can be independently adjusted by using two neutral density filters. The orthogonally polarized FW and SH pulses were afterwards collinearly recombined by using another dichroic mirror. A motorized delay stage in the FW arm was employed to temporally synchronize the FW and SH pulses. A phase-locking system based on the spatial interference of a reference continuum-wave laser at 532 nm was employed [34, 35] in our experiment to stabilize and adjust the relative phase  $\phi_L$  of the OTC pulse by using a piezo-based delay stage in the SH arm. The OTC pulses were then focused onto a supersonic gas jet of a mixture of 50% Ar and 50%  $N_2$  by a concave reflection mirror ( $f = 75$  mm) inside the apparatus.

## 3. Experimental results

In the following we will focus on the single and double ionization channels of  $N_2$  and Ar driven by OTC femtosecond laser pulses. To simplify the discussion, we denote the dissociative ionization channels of  $N_2$ , i.e.,  $N_2 + n\hbar\omega \rightarrow N^{q_1+} + N^{q_2+} + (q_1 + q_2)e$ , as  $(N^{q_1+}, N^{q_2+})$  where  $q_1$  and  $q_2$  are the charge states of the ejected fragmentations. To reveal the accessing route of the double ionization channels [2–4], we trace the dependence of the yield ratios of  $(N^+, N^+)/N_2^+$  and  $N_2^{2+}/N_2^+$  on the relative intensity between the SH and FW components of the OTC fields, i.e.,  $I_{SH}/I_{FW}$ . Since the yield of the dissociative single ionization channel  $(N^+, N)$  is only 7% compared to that of the non-dissociative  $N_2^+$  channel, the double to single ionization yield ratios are not noticeably altered whether the  $(N^+, N)$  channel is included or not. In the experiment, the combined electric field amplitude was fixed corresponds to an intensity of  $3.2 \times 10^{14} \text{ W cm}^{-2}$ . The intensities of the FW and

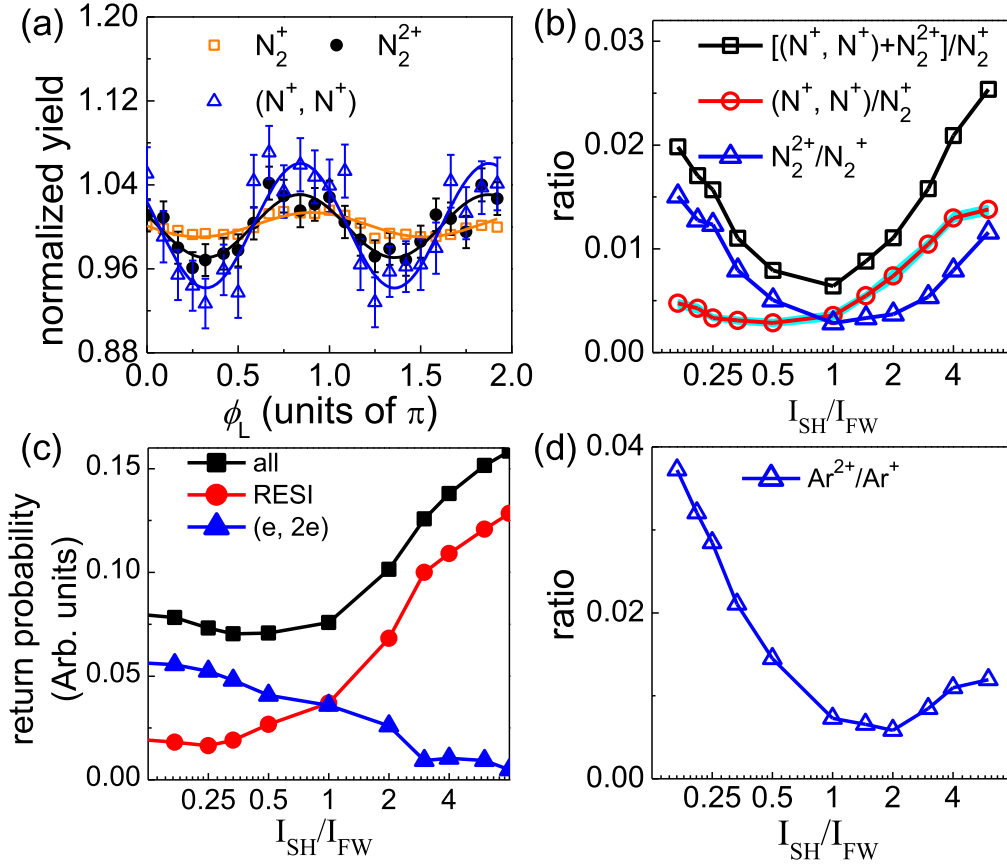


**Figure 2.** (a) Measured ion yields of  $N_2^+$  (orange squares),  $N_2^{2+}$  (black circles), and  $(N^+, N^+)$  (blue triangles) as a function of  $\phi_L$ , the orange, black and blue curves are the corresponding fitting results with sine functions, respectively. The yield ratios of (b)  $(N^+, N^+)/N_2^+$  (red circles, the cyan region is the deviation from the influence of the relative phase  $\phi_L$ ),  $N_2^{2+}/N_2^+$  (blue triangles), and  $[(N^+, N^+) + N_2^{2+}]/N_2^+$  (black squares) and (d)  $Ar^{2+}/Ar^+$  as a function of  $I_{SH}/I_{FW}$  with a maximum combined intensity of  $\sim 3.2 \times 10^{14} \text{ W cm}^{-2}$ . (c) Numerically simulated RESI probability (red circles),  $(e, 2e)$  recollision probability (blue triangles), and their sum recollision probability (black squares) as a function of  $I_{SH}/I_{FW}$ .

SH fields were calibrated by the time-of-flight spectra of  $H_2$  [36] and the yield ratio of  $Ar^{2+}/Ar^+$  [37], respectively. The relative intensities of the FW and the SH were adjusted by tuning the neutral density filters in the corresponding arms of the interferometer.

In collinearly polarized two-color laser fields, the recollision-induced processes highly depend on the relative phase of the two-color components. To examine this characteristics in an OTC field, we illustrate the yields (normalized to the mean yields of all the phases) of  $N_2^+$ ,  $N_2^{2+}$  and  $(N^+, N^+)$  as a function of the relative phase  $\phi_L$  at  $I_{SH}/I_{FW} = 0.33$  as an example. Figure 2(a) shows that the yields oscillate with a period of  $\pi$  with modulation depths around 2%, 6% and 12% for  $N_2^+$ ,  $N_2^{2+}$  and  $(N^+, N^+)$ , respectively. The  $(N^+, N^+)/N_2^+$  and  $N_2^{2+}/N_2^+$  ratios as a function of the intensity ratio shown in figure 2(b) is deviated by around 4%–13% when the relative phase between the FW and SH is varied. However, the overall tendency is not affected. Here we focus on the effect of electron recollision in non-dissociative and Coulomb explosion double ionization channels and ignore the relative phase effect in the following discussions.

Figure 2(b) shows the measured yield ratios of different double ionization channels to the single ionization channel as a function of  $I_{SH}/I_{FW}$ . The ratio of  $[(N^+, N^+) + N_2^{2+}]/N_2^+$

(black squares, the yield of double to single ionization of  $N_2$ ) exhibits a ‘V-shape’ dependence on the intensity ratio with a minimum point at around  $I_{SH}/I_{FW} \sim 1$ . This ‘V-shape’ dependence indicates the double ionization of  $N_2$  undergoes a NSDI process [38, 39]. The OTC electrical field evolves in a rotation manner depending on the phase offsets and the relative intensities between the SH and the FW components. Therefore it is not surprising that when the intensities are equal for both colors the probability of driving the electron back to its origin is much smaller than for higher and lower intensity ratios. Interestingly, as shown in figure 2(b), the  $(N^+, N^+)/N_2^+$  (red circles) and  $N_2^{2+}/N_2^+$  (blue triangles) exhibit distinct dependences on  $I_{SH}/I_{FW}$ . As compared to the  $N_2^{2+}/N_2^+$ , the  $(N^+, N^+)/N_2^+$  weakly depends on  $I_{SH}/I_{FW}$  when SH field is weaker than the FW field, and increases rapidly for  $I_{SH}/I_{FW} > 1$ . This indicates different quantum routes may contribute in producing the  $N_2^{2+}$  and  $(N^+, N^+)$  channels. In general, the tunneling and rescattering are favored at longer wavelengths. This applies for the cases with lower ratios of  $I_{SH}/I_{FW}$  when more red components exist in the OTC fields.

The angle-integrated kinetic energy releases (KERs) of the  $(N^+, N^+)$  channel is illustrated in figure 3. The yield of high KER region is distinctly increased for  $I_{SH}/I_{FW} < 1$

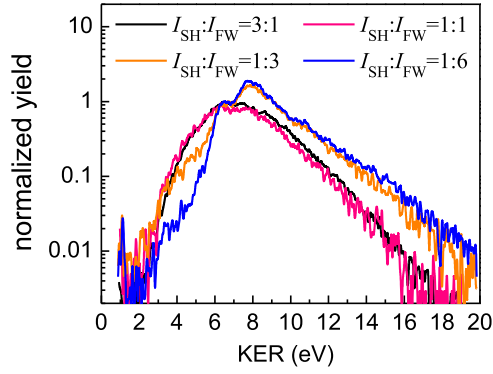


**Figure 3.** KER spectra of ( $N^+$ ,  $N^+$ ) channel produced by OTC pulse with various intensity ratios of  $I_{SH}/I_{FW}$ . The KER spectra are normalized to the yield at KER = 6.35 eV.

compared to the cases when  $I_{SH}/I_{FW} > 1$ . For explosive double ionization with a Coulomb potential of  $1/R$  (in atomic units), the high KER region (9–12 eV) is from the immediate Coulomb explosion near the equilibrium internuclear distance for the ground states of  $N_2$  (2.1–3.0 a.u.) and low KER region (4–6 eV) comes from soft Coulomb explosion at a stretched internuclear separation (4.5–6.8 a.u.). Driven by OTC laser fields, the maximum rescattering electron energy, which is scaled by the ponderomotive energy ( $U_p$ ), decreases as  $I_{SH}/I_{FW}$  grows.  $U_p$  is an important criteria for ( $e$ ,  $2e$ ) and RESI processes. NSDI prefers to be accessed through an ( $e$ ,  $2e$ ) rather than RESI mechanism for higher  $U_p$ . Assuming the ( $N^+$ ,  $N^+$ ) channel is dominated by the NSDI, the high KER region is associated with the ( $e$ ,  $2e$ ) channel (immediate Coulomb explosion) and the low KER region we attribute to RESI (soft Coulomb explosion). This assumption is consistent with the yield distinctly increasing for  $I_{SH}/I_{FW} < 1$  in the high KER region as shown in figure 3. In the RESI picture, the ground state  $N_2^+$  from tunneling ionization of a neutral molecule is firstly excited to the unstable excitation state by the electron recollision igniting the stretch of the bond length. The second electron subsequently ionizes at a larger internuclear distance. On the other hand, the enhanced high KER region of the ( $N^+$ ,  $N^+$ ) channel is dominated by ( $e$ ,  $2e$ ) impact ionization, where the  $N_2$  molecule Coulomb explodes at a rarely stretched bond length. According to the higher  $N_2^{2+}/N_2^+$  yield ratio compared to ( $N^+$ ,  $N^+$ )/ $N_2^+$  for  $I_{SH}/I_{FW} < 1$  as shown in figure 2(b), we infer the  $N_2^{2+}$  channel is dominated by ( $e$ ,  $2e$ ) impact ionization while the ( $N^+$ ,  $N^+$ ) channel is accessed via the RESI at a large internuclear distance.

#### 4. Numerical simulations

To strengthen our understanding of the rescattering-assisted double ionization process, classical trajectory Monte Carlo simulations were performed using a spherical potential by numerically solving two-dimensional Newton's equations of motion for the liberated electrons in the OTC fields. The superimposed electric field can be written as  $\mathbf{E}(t) = E_y(t) \hat{\mathbf{e}}_y + E_z(t) \hat{\mathbf{e}}_z = f_y(t) \cos(\omega t) \hat{\mathbf{e}}_y + f_z(t) \cos(2\omega t + \phi_L) \hat{\mathbf{e}}_z$ .

According to the Ammosov–Delone–Krainov theory [40, 41], an electron is released with the initial location given by  $\mathbf{r} = y \hat{\mathbf{e}}_y + z \hat{\mathbf{e}}_z = -I_p/|\mathbf{E}(t)|^2 [E_y(t) \hat{\mathbf{e}}_y + E_z(t) \hat{\mathbf{e}}_z]$ , and with zero longitudinal momentum and Gaussian transverse momentum distributions. The single ionization potential of  $N_2$  is  $I_p = 15.6$  eV. The liberated electron propagates in the remaining laser electric field and the modeled potential of  $V(y, z) = -1/(y^2 + z^2 + \alpha)^{1/2}$  with single Coulombic center at the original point. The soft-core parameter was set at  $\alpha = 0.6$ . We traced the electron movement, and recorded the electron energy when it returns to the parent ion with a distance smaller than 5 a.u., which can potentially lead to the double ionizations induced by recollision. More than  $10^7$  electron trajectories emitted at different instants within the OTC pulses were launched in our calculations for each phase  $\phi_L = 0.125n\pi$ , where  $n = 1, 2, 3 \dots 16$ . Figure 4 displays the calculated returning energy spectra of the liberated electrons for various laser intensity ratios. As expected, the simulated results indicate that a higher  $I_{SH}/I_{FW}$  is accompanied with a lower recolliding energy, which could lead to the RESI pathway. In figure 4, the green dashed vertical lines denote the energy required for the ( $e$ ,  $2e$ ) double ionization channel ( $\sim 27.1$  eV) to occur. The events below 27.1 eV are integrated as the RESI probability and the yields of those exceeding 27.1 eV are integrated for the ( $e$ ,  $2e$ ) probability. The estimated RESI and ( $e$ ,  $2e$ ) impact ionization probabilities are presented in figure 2(c) by the red circles and the blue triangles, respectively. The simulation curve indicates a ‘V-shape’ dependency for the NSDI channel, which reproduces the experimental observations qualitatively. The model is consistent with a dominant RESI mechanism for the ( $N^+$ ,  $N^+$ ) channel and an ( $e$ ,  $2e$ ) impact ionization mechanism for the  $N_2^{2+}$  channel.

#### 5. Discussions

According to the simulation results, the returning energy of the rescattered electrons increases with the decreasing of  $I_{SH}/I_{FW}$ . And the internuclear distance at the instant of electron's birth in the ionization process affect the quantum pathways. For the ( $e$ ,  $2e$ ) impact double ionization channel, the two electrons are released simultaneously which indicates the molecular internuclear distance is frozen near the equilibrium position during the ionization process. If the two electrons are kicked out from the outmost orbital, the double ionization will probably produce  $N_2^{2+}$  channel. Supposing that one electron is released from the outmost orbital and the second electron is kicked out afterwards from an inner orbital or the two electrons are both released from inner orbitals, it is more probable to get the ( $N^+$ ,  $N^+$ ) channel with KER distributions at higher energies, which agrees with our observations. Furthermore, the experimental results proved that the double ionization of Ar in this OTC fields is attributed to the ( $e$ ,  $2e$ ) impact double ionization since the  $Ar^{2+}/Ar^+$  channel shows a similar ratio dependence comparing to the  $N_2^{2+}/N_2^+$  channel which both represents atomic-like behavior, as illustrated in figure 2(d). For the RESI channel, the  $N_2^+$  would

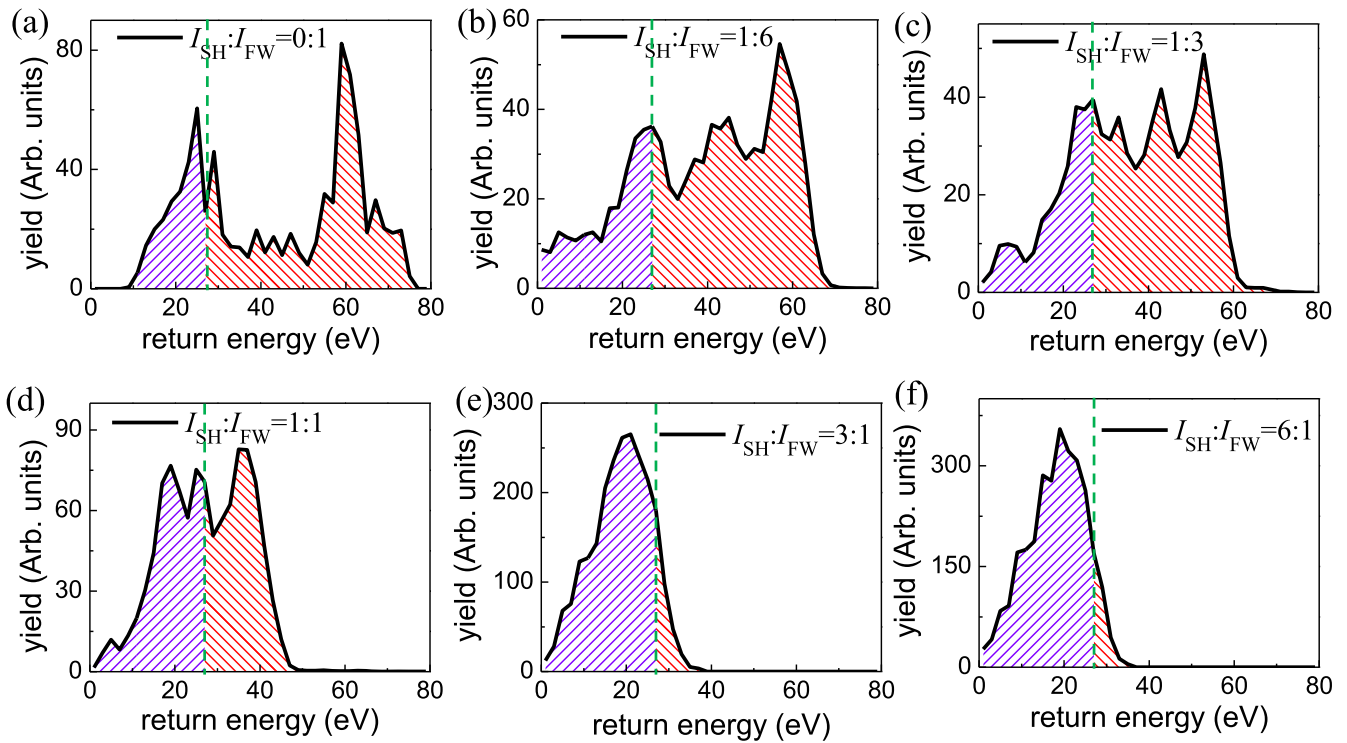


**Figure 4.** Simulated electron recolliding energy spectra at different field intensity ratios of  $I_{SH}/I_{FW}$ . The recolliding energy needed for ( $e$ ,  $2e$ ) double ionization at 27.1 eV is marked with a green dashed line.

stay on an excited state after the recollision by the first electron. In multicycle femtosecond laser fields, there is enough time for the cations to stretch their internuclear distances after the ionization of the first electron. If the internuclear distance has expanded when the second electron is tunneled in the subsequent laser field, it would result in a dissociative double ionization with a low KER. Apparently, the stretched internuclear distance enhanced the ionization rate for the ( $N^+$ ,  $N^+$ ) channel. Moreover, the experimental and numerical results for the  $N_2^{2+}/N_2^+$  channel show different dependences for high  $I_{SH}/I_{FW}$ , this can be due to the fact that the resonant multiphoton ionization was not included in the numerical simulations, which also play a role in the double ionization process, especially for  $I_{SH}/I_{FW} > 1$ .

## 6. Conclusion

To summarize, we investigated the double ionization of  $N_2$  and Ar in OTC femtosecond laser fields under different intensity ratios between the FW and its SH components. The yield ratios of different double ionization channels, i.e., the non-dissociative  $N_2^{2+}$  and Coulomb exploded ( $N^+$ ,  $N^+$ ), to the singly charged  $N_2^+$  channel exhibit distinct dependences on the relative intensity  $I_{SH}/I_{FW}$ . As  $I_{SH}/I_{FW}$  increases, the yield ratio of ( $N^+$  +  $N^+$ )/ $N_2^+$  gradually increases, but the yield ratio of  $N_2^{2+}/N_2^+$  first descends and then increases with a minima which is similar to the behavior for  $Ar^{2+}/Ar^+$ . By tracing the returning energy of the recolliding electrons in classical trajectory simulations, we find that the non-dissociative double ionization channel is dominated by the

( $e$ ,  $2e$ ) impact ionization while the Coulomb exploded ( $N^+$ ,  $N^+$ ) channel is attributed to the RESI. By varying relative intensity of the two colors of an OTC ultrashort laser pulse, the accessibility of different ionization pathways in strong-field NSDI can be manipulated. This provides a promising tool for the coherent control of strong-field ionization processes.

## Acknowledgments

This work is supported by the National Natural Science Foundation of China (Grants Nos. 11704124, 11425416, 61690224, 11621404, 11322438, 11574205, 11421064, 11761141004), the 111 project of China (Grant No. B12024), and the Shanghai Sailing Program (Grants No. 17YF1404000).

## ORCID iDs

Qiyong Song  <https://orcid.org/0000-0001-8303-1889>  
Xiaochun Gong  <https://orcid.org/0000-0002-4826-6049>

## References

- [1] L'Huillier A, Lompre L A, Mainfray G and Manus C 1983 *Phys. Rev. A* **27** 2503–12
- [2] Walker B, Sheehy B, DiMauro L F, Agostini P, Schafer K J and Kulander K C 1994 *Phys. Rev. Lett.* **73** 1227–30

- [3] Guo C, Li M, Nibarger J P and Gibson G N 1998 *Phys. Rev. A* **58** R4271–4 (R)
- [4] Guo C and Gibson G N 2001 *Phys. Rev. A* **63** 040701(R)
- [5] Staudte A *et al* 2007 *Phys. Rev. Lett.* **99** 263002
- [6] Zhou Y, Liao Q, Zhang Q, Hong W and Lu P 2010 *Opt. Express* **18** 632–8
- [7] de Morisson Faria C F and Liu X 2011 *J. Mod. Opt.* **58** 1076–131
- [8] Camus N *et al* 2012 *Phys. Rev. Lett.* **108** 073003
- [9] Bergues B *et al* 2012 *Nat. Commun.* **3** 813
- [10] Zhang L *et al* 2014 *Phys. Rev. Lett.* **112** 193002
- [11] Corkum P B 1993 *Phys. Rev. Lett.* **71** 1994–7
- [12] Becker W, Liu X, Jo Ho P and Eberly J H 2012 *Rev. Mod. Phys.* **84** 1011–43
- [13] Xie X *et al* 2012 *Phys. Rev. Lett.* **109** 243001
- [14] Guo C, Li M and Gibson G 1999 *Phys. Rev. Lett.* **82** 2492–5
- [15] Alnaser A S, Maharjan C M, Tong X M, Ulrich B, Ranitovic P, Shan B, Chang Z, Lin C D, Cocke C L and Litvinyuk I V 2005 *Phys. Rev. A* **71** 031403(R)
- [16] Betsch K J, Pinkham D W and Jones R R 2010 *Phys. Rev. Lett.* **105** 223002
- [17] Kling N G, McKenna J, Sayler A M, Gaire B, Zohrabi M, Ablikim U, Carnes K D and Ben-Itzhak I 2013 *Phys. Rev. A* **87** 013418
- [18] Lai W and Guo C 2015 *Phys. Rev. A* **92** 013402
- [19] Kitzler M and Lezius M 2005 *Phys. Rev. Lett.* **95** 253001
- [20] Kitzler M, Xie X, Scrinzi A and Baltuska A 2007 *Phys. Rev. A* **76** 011801
- [21] Kim C M, Kim I J and Nam C H 2005 *Phys. Rev. A* **72** 33817
- [22] Ruiz C, Hoffmann D J, Torres R, Chipperfield L E and Marangos J P 2009 *New J. Phys.* **11** 113045
- [23] Shafir D, Mairesse Y, Villeneuve D M, Corkum P B and Dudovich N 2009 *Nat. Phys.* **5** 412–6
- [24] Niikura H, Dudovich N, Villeneuve D M and Corkum P B 2010 *Phys. Rev. Lett.* **105** 053003
- [25] Murray R, Ruiz C, Marangos J P and Ivanov M Y 2010 *J. Phys. B: At. Mol. Opt. Phys.* **43** 135601
- [26] Zhou Y, Huang C, Tong A, Liao Q and Lu P 2011 *Opt. Express* **19** 2301–8
- [27] Gong X, He P, Song Q, Ji Q, Pan H, Ding J, He F, Zeng H and Wu J 2014 *Phys. Rev. Lett.* **113** 203001
- [28] Song Q, Lu P, Gong X, Ji Q, Lin K, Zhang W, Ma J, Zeng H and Wu J 2017 *Phys. Rev. A* **95** 013406
- [29] Li H, Gong X, Lin K, de Vivie-Riedle R, Tong X M, Wu J and Kling M F 2017 *J. Phys. B: At. Mol. Opt. Phys.* **50** 172001
- [30] Gong X *et al* 2017 *Phys. Rev. Lett.* **118** 143203
- [31] Geng J-W, Xiong W-H, Xiao X-R, Peng L-Y and Gong Q 2015 *Phys. Rev. Lett.* **115** 193001
- [32] Dörner R, Mergel V, Jagutzki O, Spielberger L, Ullrich J, Moshhammer R and Schmidt-Böcking H 2000 *Phys. Rep.* **330** 95–192
- [33] Ullrich J, Moshhammer R, Dorn A, Dörner R, Schmidt L, Ph H and Schmidt-Böcking H 2003 *Rep. Prog. Phys.* **66** 1463–545
- [34] Mashiko H, Gilbertson S, Li C, Khan S D, Shakya M M, Moon E and Chang Z 2008 *Phys. Rev. Lett.* **100** 103906
- [35] Chini M, Mashiko H, Wang H, Chen S, Yun C, Scott S, Gilbertson S and Chang Z 2009 *Opt. Express* **17** 21459–64
- [36] Alnaser A S, Tong X M, Osipov T, Voss S, Maharjan C M, Shan B, Chang Z and Cocke C L 2004 *Phys. Rev. A* **70** 023413
- [37] Henrichs K *et al* 2013 *Phys. Rev. Lett.* **111** 113003
- [38] Mancuso C A *et al* 2016 *Phys. Rev. Lett.* **117** 133201
- [39] Eckart S *et al* 2016 *Phys. Rev. Lett.* **117** 133202
- [40] Landau L D and Lifshitz E M 1977 *Quantum Mechanics* (Oxford: Pergamon)
- [41] Liu M-M, Li M, Wu C, Gong Q, Staudte A and Liu Y 2016 *Phys. Rev. Lett.* **116** 163004